



A novel colorimetric sensor array for real-time and on-site monitoring of meat freshness

Wengui Nie¹ · Yifei Chen¹ · Hua Zhang¹ · Jinsen Liu² · Zhengchun Peng³ · Yingchun Li^{3,4}

Received: 22 March 2022 / Revised: 5 May 2022 / Accepted: 13 June 2022 / Published online: 5 July 2022
© Springer-Verlag GmbH Germany, part of Springer Nature 2022

Abstract

Food quality control is essential in industry and daily life. In this work, we developed a novel colorimetric sensor array composed of several pH-sensitive dyes for monitoring meat freshness. A color change in the sensor array was seen after exposure to volatile organic compounds (VOCs), and the images were captured for precise quantification of the VOCs. In conjunction with pattern recognition, meat freshness at different storage periods was readily discerned, revealing that the as-fabricated colorimetric sensor array possessed excellent discrimination ability. The linear range for quantitative analysis of volatiles related to meat spoilage was from 5 ppm to 100 ppm, with a limit of detection at the ppb level ($S/N = 3$). Furthermore, the testing results obtained by the sensor in assessing meat freshness were validated by a standard method for measuring the total volatile basic nitrogen (TVB-N). The sensing signals showed good agreement with the results obtained in TVB-N when measuring real food samples. The sensor also displayed good reproducibility ($RSD < 5\%$) and long-term stability. The sensor was successfully used for on-site and real-time determination of volatiles emitted from rotting meat, demonstrating its potential application in monitoring the quality and safety of meat products.

Keywords Visualization · Volatile organic compounds (VOCs) · TVB-N · Biogenic amines · Meat freshness

Introduction

With the rapid development of the social economy and the gradual improvement of living standards, consumers have developed a growing awareness of product quality in the food industry. Meats are rich in high-quality protein and

lipids [1, 2], which are also favorable nutrient sources for microbes. Meat spoilage leads to the production of amines, organic acids, sulfides, and unpleasant off-flavors due to the growth of microorganisms [3]. Meat spoilage not only causes deterioration in quality and diminishes nutritional value, but also may endanger the health of consumers. Therefore, the development of highly facile and reliable techniques for monitoring meat freshness during transportation, storage, and processing is of great importance.

Most of the currently employed analytical techniques for monitoring food quality, such as gas chromatography–mass spectrometry (GC-MS) [4, 5], Fourier transform infrared spectroscopy (FT-IR) [6, 7], Raman spectroscopy [8], and chemiluminescence [9, 10], require sophisticated instrumentation. Additionally, they often suffer from complicated operation, high cost, time-consuming protocols, lack of portability, and the need for qualified personnel, which limits their application for real-time and on-site determination. To this end, rapid, cost-effective, operation-friendly, nondestructive, and even online detection of meat freshness is particularly important for the regulation of meat quality and safety.

Wengui Nie and Yifei Chen contributed equally to this work.

✉ Zhengchun Peng
zcpeng@szu.edu.cn

✉ Yingchun Li
liyinchun@hit.edu.cn

¹ Key Laboratory of Xinjiang Phytomedicine Resources for Ministry of Education, School of Pharmacy, Shihezi University, Shihezi 832000, China

² Shenzhen ENCO Instrument Co., Ltd, Shenzhen 518000, China

³ School of Physics and Optoelectronic Engineering, Shenzhen University, Shenzhen 518060, China

⁴ Flexible Printed Electronics Technology Center and School of Science, Harbin Institute of Technology, Shenzhen 518055, China

With the development of bionic technology, electronic tongue (E-tongue), electronic nose (E-nose), and other rapid detection methods have been developed for assessing meat freshness [11, 12]. Among them, E-nose has attracted much attention owing to its fast and noninvasive features. However, the traditional metal oxide E-nose is susceptible to interference from environmental conditions (e.g., temperature, humidity) [13]. Besides, the weak binding force between the metal oxide and the characteristic gases of food spoilage (e.g., amines and mercaptan) results in poor sensing response.

Colorimetric sensor arrays have recently emerged as a rapid and low-cost analytical tool for use in many fields, such as food safety [14–16], biomedical diagnostics [17, 18], environmental monitoring [13, 19], chemical studies, and explosives identification [20, 21]. The inspiration for the colorimetric sensor array was drawn from the mammalian olfactory system, which is able to accurately sense trillions of scents using hundreds of olfactory receptors [22–24]. Olfactory receptors specifically bind a range of scent molecules. One odorant molecule can bind several receptors with varying affinities and activate several receptors, generating the odor fingerprint [16, 25, 26]. Correspondingly, when a colorimetric sensor array binds to an individual analyte, it creates various signals and provides a unique pattern for the identification of each analyte [13]. The construction of a colorimetric sensor array is based mainly on chemoresponsive dyes and solid supports. The selection of solid supports and immobilization methods has a significant effect on the performance of the colorimetric sensor array. Polyvinylidene difluoride (PVDF) membranes have been used as the solid support because of their homogeneous structure, low cost, and photochemical stability. For immobilization of colorimetric agents, sol–gel processing is characterized by uniform porosity, high surface area, large pore volume, and mechanical rigidity. Therefore, sol–gels are considered an excellent solid matrix to immobilize dyes. Colorimetric sensor arrays feature rapid visualization, high specificity, cost-effectiveness, simplicity, and portability. In terms of the assessment of food quality, the colorimetric sensor array has been employed to monitor solid food including rice [27, 28], fish [29, 30], chicken [31], and pork [32], and liquid foods like Chinese liquors [33], vinegar [34], and milk [35].

In this work, a cross-responsive sensor array was prepared and used for real-time meat freshness detection, the design of which is mainly based on colorimetric reactions between the volatile compounds released from meat samples (e.g., biogenic amines, sulfides) and the selected dyes. The colorimetric sensor array was prepared using a PVDF membrane as the flexible substrate, and the colorimetric dyes were first immobilized by sol–gels and then drop-coated on each sensing unit. The use of sol–gels in building a colorimetric array was attempted for the first time. The sensor array was

used for the quantification of four representative volatiles in rotting meat. Data acquired from the sensor array were processed with hierarchical cluster analysis (HCA) and principal component analysis (PCA). Total volatile basic nitrogen (TVB-N) as a traditional freshness indicator was also measured and compared with the sensing results. Finally, the fabricated array was employed to differentiate meat freshness at different storage intervals.

Experimental section

Experimental materials and reagents

Triethoxyoctylsilane (98%), 2-methoxyethanol (99%), propylene glycol 1-monomethyl ether 2-acetate (99%), tetraethoxysilane, triethylamine (99%), dimethylamine (40 wt.%), trimethylamine (30%), cadaverine (98%) and all chemoresponsive dyes were purchased from Titan Scientific Co., Ltd. (Shanghai, China). Other chemicals including H_3BO_3 and K_2CO_3 were supplied by Greagent Reagent Co., Ltd. (Shanghai, China). The PVDF membranes (0.45 μm) were acquired from Qiguanchao (Zhejiang, China). All chemicals were of analytical grade and the solutions were prepared with distilled water.

Preparation of the sensor array

The chemical dyes and the formulations used in each spot are listed in Table S1. The table color represents the initial color of the array after printing. The 5×5 colorimetric sensor array was artificially prepared on a square polyvinylidene fluoride (PVDF) film (side length: 30 mm). For each unit, the dye solution (200 nL) was transferred to the corresponding site by drop-coating with a glass capillary. It is worth mentioning that, in order to control the distance between the sensor units, a glass mask with the expected array pattern was designed and adopted (Fig. S1a and b). The glass mask was made by Guluo Glass Co., Ltd. (Luoyang, China) using a laser cutting technique. When preparing the sensor array, the PVDF film was placed under the glass mask. Once printed, the arrays were dried for 2 h at 25 °C and stored in N_2 -filled aluminized Mylar bags before usage. The sensor arrays were aged for at least 3 days before use to maximally weaken baseline drifts. Figure S1b shows the array image taken with the scanner.

Meat sample preparation

Four types of raw meat, including fish, chicken (chicken breast fillet), beef (beef sirloin), and pork (pork tenderloin), were supplied by a local supermarket and tested during storage. Ten-gram meat samples were placed in a 200 mL

polypropylene plastic box with a lid. Meat samples were stored at room temperature (25 °C) or in a refrigerator (4 °C). To investigate the influence of the packaging environment on meat freshness, fish samples stored in 200 mL boxes filled with N₂ were tested at room temperature. During analysis of these real samples, a container made from polypropylene was adopted for placement of the sensor array (Fig. S2). The container was attached to the inner side of the box lid. It was designed with several holes (inset of Fig. S2a), allowing contact between the volatile gases from samples and the sensor array. The testing procedure for meat samples is shown in Movie S1 of the Supporting Information.

Detection of amine gases

Detection of amine gases was performed in an 18.0 L chamber at room temperature. The sensor array was placed in the gas sensor test system. The desired gas concentration was achieved by injecting a certain volume of each liquid analyte into the system. The resulting gas concentration (*C*) was calculated using the following formula,

$$C = \frac{V \times D \times W}{M \times V_0} \times 22.4 \times 10^{-9} \quad (1)$$

where *V* (μL) is the liquid analyte volume, *D* (mg/L) is the liquid density, *W* is the mass fraction of the liquid, *M* (g/mol) is the molecular weight of the liquid analyte, and *V*₀ (L) is the chamber volume.

TVB-N analysis

The TVB-N level of meat samples was measured by the micro-diffusion method [16]. Details are as follows: The meat sample (10 g) and distilled water (100 mL) were homogenized by a homogenizer (Deerma, JS200, 40 W) for an interval of 5 min, and then the mixture was filtered through a 60 mesh filter to obtain a sample liquid. Then, 3 mL boric acid solution (20 g/L) and 50 μL pH indicator (methyl red/bromocresol green = 1:5, V/V) were added to the inner part of the Conway dish. Saturated potassium carbonate solution (3 mL) and sample solution (1 mL) were added to the outer chamber in sequence. The Conway dish was sealed and left at 37 °C for 2 h. Afterwards, the boric acid solution was titrated with 0.01 M hydrochloric acid (HCl) solution. The TVB-N value was determined by the amount of HCl consumed and expressed in units of mg/100 g.

Signal extraction and data analysis of colorimetric sensor array

For analysis of each meat sample, a flatbed scanner (Epson V370) was employed to capture the images of the array

before and after analyte exposure. The images were then processed with color measurement software written by Huhui Technology Co., Ltd. (Wuhan, China). The data analysis software is based on the same principle as the usual Photoshop and ImageJ, which can read out red, green, and blue (RGB) values of each colorimetric unit, and then calculate changes in the RGB color values of each element of the array by subtracting the averaged color intensity of each element before and after exposure to the analyte [36], as shown in Eqs. (2)–(4). Subtraction of the two images yielded a difference vector of 3*N* dimensions, where *N* is the total number of spots (25 [dyes] × 3 [color component difference] = 75 dimensions). The Euclidean distance (*ED*) of RGB values for each sensing unit before and after exposure to the volatile organic compounds (VOCs) was calculated with Eq. (5). In order to clearly display the color change, the color difference range was set at 0–255. The data were analyzed by PCA and HCA.

$$\Delta R = |R_{after} - R_{before}| \quad (2)$$

$$\Delta G = |G_{after} - G_{before}| \quad (3)$$

$$\Delta B = |B_{after} - B_{before}| \quad (4)$$

$$ED = \sqrt{(\Delta R)^2 + (\Delta G)^2 + (\Delta B)^2} \quad (5)$$

Results and discussion

Sensor response to gas analytes

During meat storage, owing to the effects of tissue enzymes, external microorganisms, and other factors, changes in meat composition take place, resulting in the deterioration and rotting of the meat. The process accompanies the generation of short-chain alcohols, biological amines (e.g., ammonia and trimethylamine), sulfur-bearing volatile substances, etc. These volatile compounds can act as markers to indicate the freshness and spoilage stage of meat products. Here, we tested the responses of our colorimetric sensor array towards multiple freshness-related gases, including ammonia (NH₃), trimethylamine (TMA), dimethylamine (DMA), and cadaverine (CAD). Generally, the selection of chemo-responsive dyes is based on whether they contain an interaction center that can interact strongly with the analyte. Here, the colorimetric sensor array is composed of Brønsted acidic dyes (sulfonphthaleine in this work), Brønsted basic dyes (crystal violet and basic fuchsin), and Lewis acid dyes (porphyrins).

For the sulfonphthaleine dyes, when exposed to VOCs, deprotonation leads to rearrangement of the internal bonds, further resulting in a larger conjugated structure and a free SO_3^- group (Fig. S3a). As for the Brønsted basic dyes, they can combine with the acidic substances (e.g. H_2S), leading to a change in color. In addition, it is well recognized that Lewis acid dyes show significant solvatochromic effects, resulting in distinguishable colorimetric differences before and after interactions with VOCs [37, 38].

A typical sensing response of the constructed colorimetric sensor array after exposure to DMA is shown in Fig. S3b, and the corresponding color difference map is illustrated in Fig. S3c, which indicates that biogenic amine gas can react with the abovementioned dyes and generate different color changes. Figure S4 shows the response of the array to 25 ppm DMA gas as a function of time, indicating that the response reaches equilibrium after 4 min. Thus, the response time was set at 4 min and used in the following colorimetric assays. The overall color difference maps after exposure to the above four gas analytes are presented in Fig. 1. Color changes are clearly observed for all amine gases at ppm concentration, and the patterns allow for easy differentiation even by the naked eye.

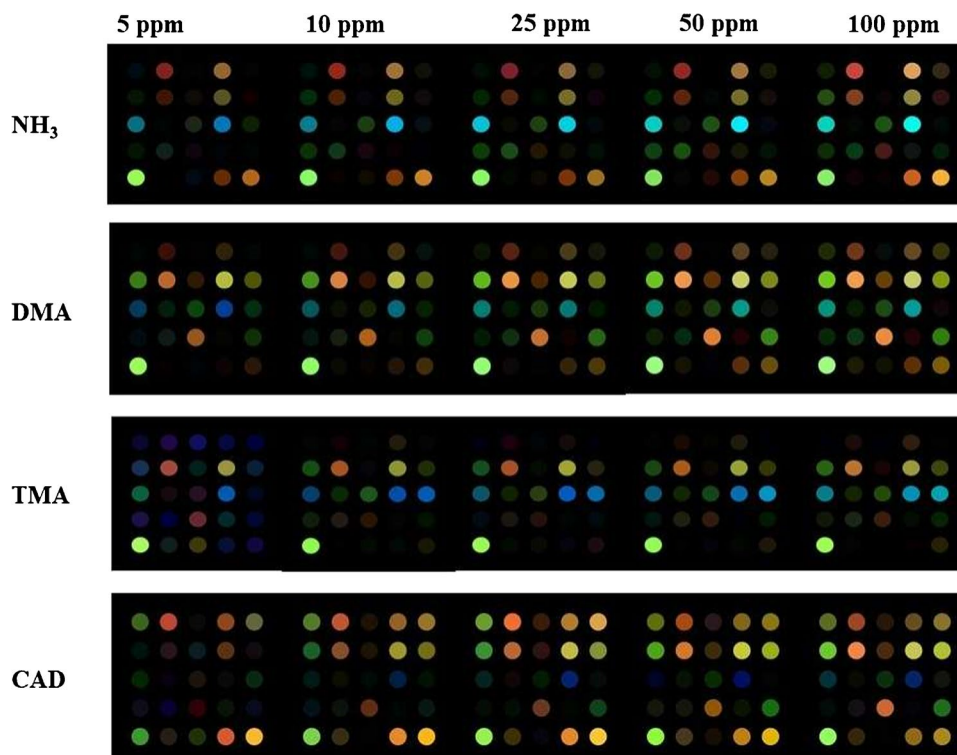
To evaluate the performance of the sensor array in discriminating the amines, the collected sensing data were processed by HCA and PCA, both of which are unsupervised exploratory data analyses [33, 39]. PCA is a data dimensionality reduction technique that can reveal the scale of the

chemical active space detected by the array, while HCA is normally used to evaluate the similarity/dissimilarity among data points and cluster them in multivariate vector space [14, 15, 40].

PCA was used to provide an estimation of the dimensionality of the colorimetric sensor array data, which is a measure of the dimensionality of a wide range of chemical properties space probed by the sensor array [41]. As shown in Fig. 2a, the three-dimensional (3D) score plot of PCA using the first three principal components (accounting for 71.9% of the total variance) shows that clusters of four volatiles are clearly separated. From the PCA scree plot (Fig. 2b), one can see that a total of 10 principal components (PCs) were still required to account for 90% of the total variance and 16 PCs for 95%. This may be due to the high similarity in alkalinity and structure of the tested amine molecules. Also, it may be that some information in the original data was not considered by the first three principal components. Both of these could result in poor clustering results [37, 42].

HCA groups data using a distance metric and a clustering criterion in multidimensional space. The main parameters we chose were the Euclidean distance and Ward's method. Ward's method is used to define the linkage between the clusters which is the minimum amount of the variance between the samples [42]. In this method, the nearest-neighbor points are paired into a single cluster, which is then paired with other nearest-neighbor points or clusters until all points and clusters are connected to

Fig. 1 Sensor array responses of VOCs towards 5–100 ppm (a) NH_3 , (b) DMA, (c) TMA and (d) CAD



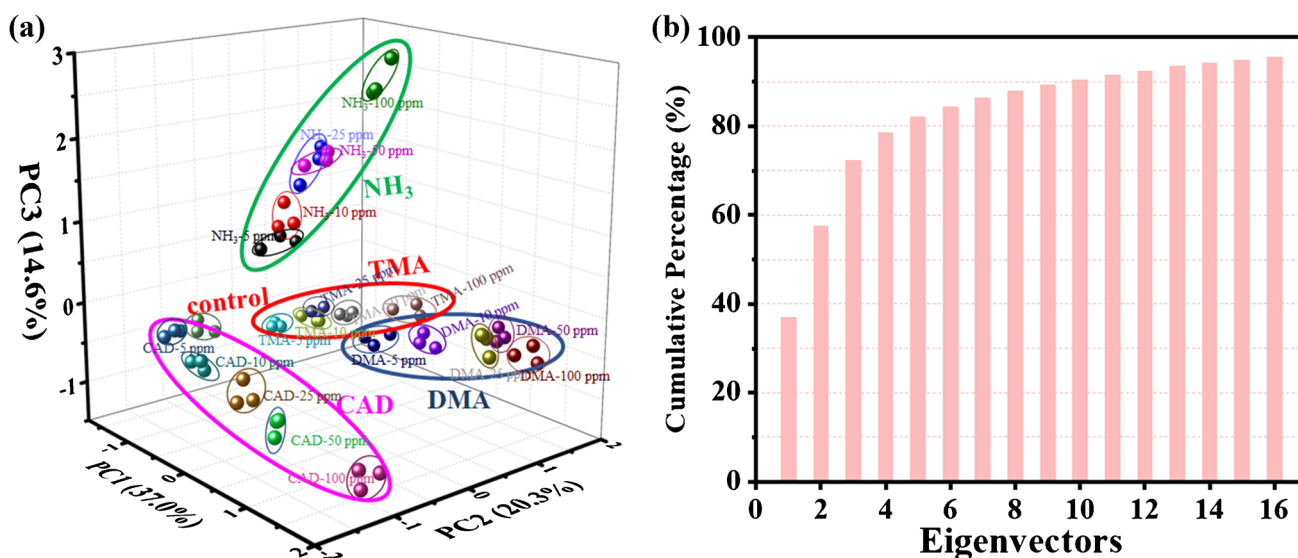


Fig. 2 **a** 3D PCA score plot based on the concentrations (5–100 ppm) of four VOCs. **b** Scree plot of the distribution of the total variance of each principal component

each other [37, 43]. The clustering results of HCA give a similar pattern, in agreement with the score plot of PCA based on the three PCs with no overlap among clusters. The resulting HCA dendrogram of the four VOCs at five concentrations is shown in Fig. 3. The generated cluster tree showed the four amine gases formed clear separate clusters between 5 ppm and 100 ppm. Overall, each sample is discriminable without confusion or error, except for one subgroup (DMA at 5 ppm). As seen in Fig. S5 and Table S2, the limits of detection (LOD) for NH₃, TMA, DMA, and CAD are below 20 ppb ($S/N = 3$).

Monitoring of meat freshness

Effective monitoring of food freshness is important to guarantee food safety. In this work, the constructed colorimetric sensor array was used to evaluate the freshness of four kinds of meat (fish, pork, chicken, and beef). It is worth mentioning that we designed a sensor container made from an inert material-polypropylene, aimed at avoiding direct contact between the meat and the sensor. As we know, polypropylene is widely used for food packaging owing to its great stability and safety. Biogenic amines can permeate the array through the holes and induce color reactions. Figure 4 shows the color maps obtained from the array in monitoring the four kinds of meat stored at 25 °C for 72 h. An apparent color change can be observed during the monitoring processes (Movie S2, Supporting Information). Furthermore, to assess the applicability of our sensor under refrigeration conditions, we put the sensor array in fish and pork packages that were stored at 4 °C, and the results are displayed in Fig. S6.

The response curves based on ED values versus storage time are illustrated in Fig. S7a. The increase in ED values is related to an increase in nitrogen compounds, which is attributed to the decomposition of proteins by microorganisms. As shown in Fig. S7b, the ED values obtained at 25 °C increased faster than those at 4 °C, as low temperature inhibits the growth and reproduction of microorganisms, thereby slowing the degradation and spoilage of protein in meat. Even at the refrigerated temperature (4 °C), however, the sensor array showed an increase in volatile concentration over time.

We further used PCA and HCA to illustrate the capability of the sensor to quantitatively assess meat freshness. As shown in Fig. 5a, the PCA score plot of the first two principal components (which only captures > 69.3% of the total variance) shows relatively good separation among the analytes, as indicated by circling obvious clusters (fresh, less fresh, and spoiled). The PCA scree plot (Fig. 5b) shows that the array required 11 and 20 dimensions to capture 90% and 95% of the total variance, respectively. These results indicate that the prepared colorimetric sensor array could detect a wide range of physical/chemical activity and demonstrated the high recognition capability of the as-fabricated sensor array for different meat samples.

As shown in Fig. 6, the HCA dendrogram based on the ED values among the collected samples shows three distinct clusters. The first cluster (fresh) contains all meat samples stored for 0 h and 4 h, chicken and beef samples for 8 h, and the control. The second cluster (less fresh) consists of all meat samples with storage of 12 h or 24 h, as well as fish and pork samples stored for 8 h. The last cluster (spoiled) is composed of most meat samples

Fig. 3 HCA dendrogram of four amine gases over the concentration range of 5–100 ppm

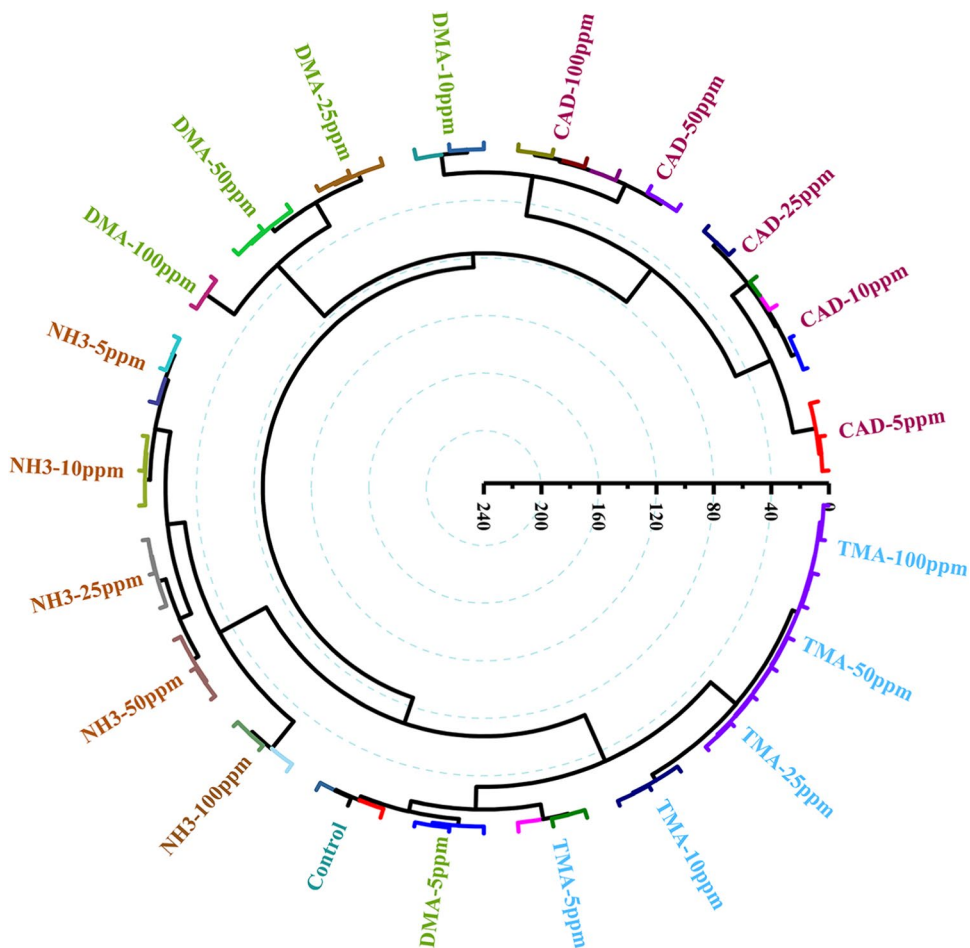
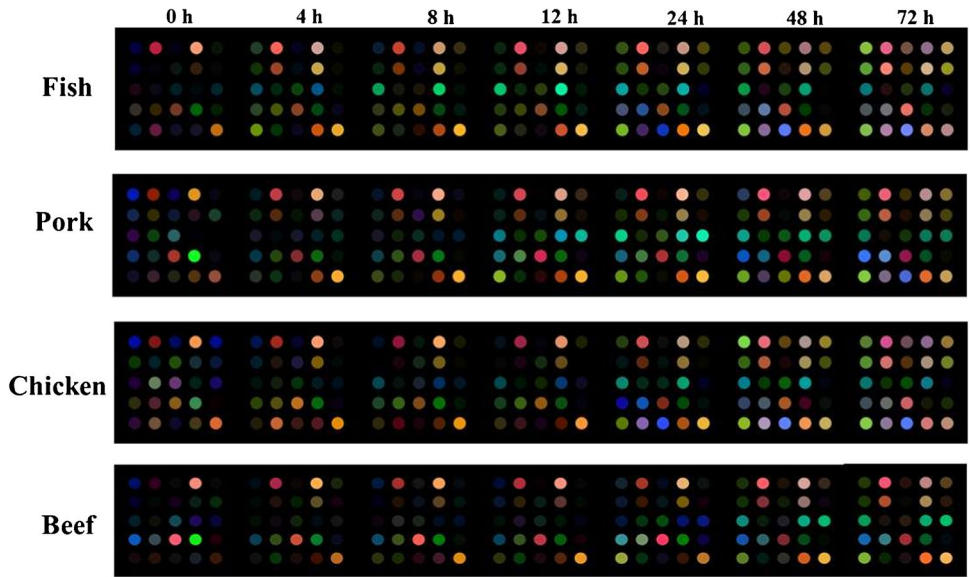


Fig. 4 Sensor array responses towards four kinds of meat including (a) fish, (b) pork, (c) chicken, and (d) beef at 25 °C during 72 h storage



with storage of 48 h and 72 h. All the meat samples are clearly clustered, except for one group containing beef stored for 72 h. The accurate clustering via HCA based on

the data collected by the sensor further demonstrated the good identification capability of our proposed colorimetric sensor array for assessing food freshness.

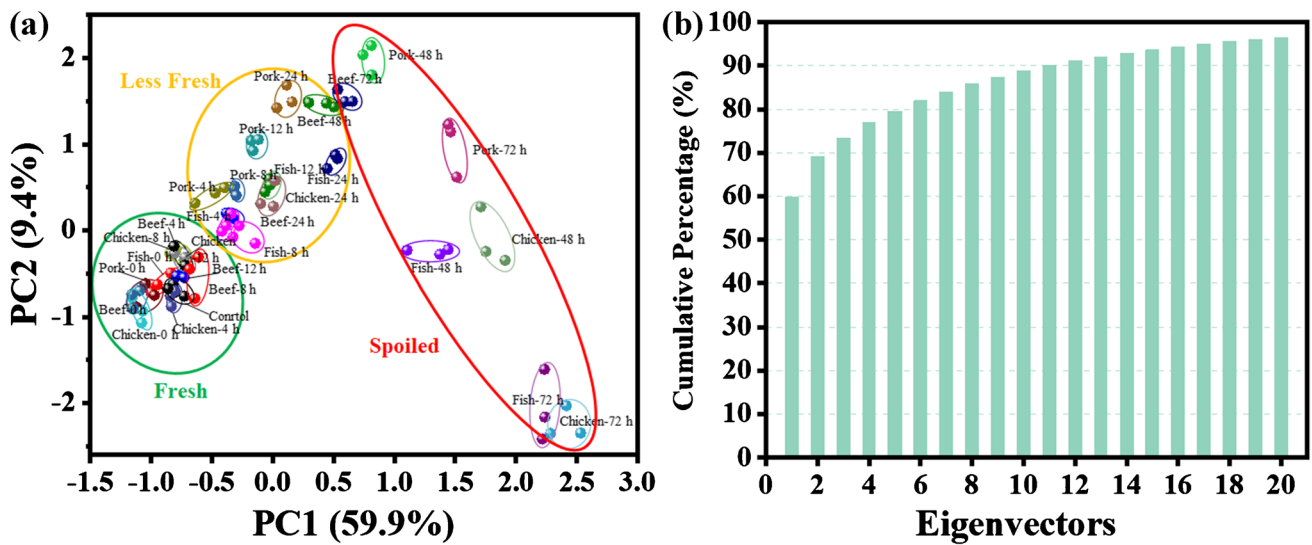
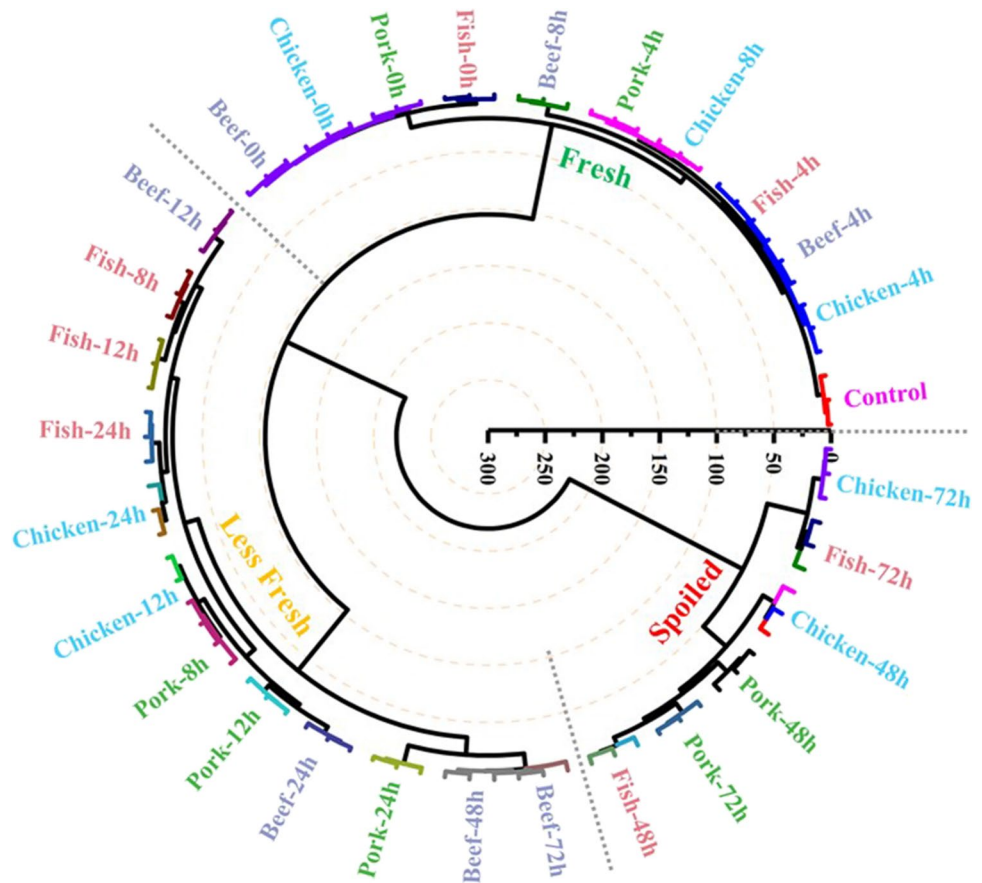


Fig. 5 a PCA score plot of the meat samples at 25 °C. b Scree plot of the distribution of the total variance of each principal component

Fig. 6 HCA dendrogram of the four types of meat stored at 25 °C



TVB-N analysis

Over time, proteins in rotting meat can be microbially decomposed into amines (ammonia, dimethylamine, trimethylamine, etc.), also known as total volatile basic nitrogen

(TVB-N). TVB-N is an important indicator used to evaluate the freshness of protein-rich foods. Generally, meat can be divided into three types based on the level of TVB-N released from 100 g meat: ≤ 15 mg for fresh meat, 15–20 mg for edible but less fresh meat, and ≥ 20 mg for meat that

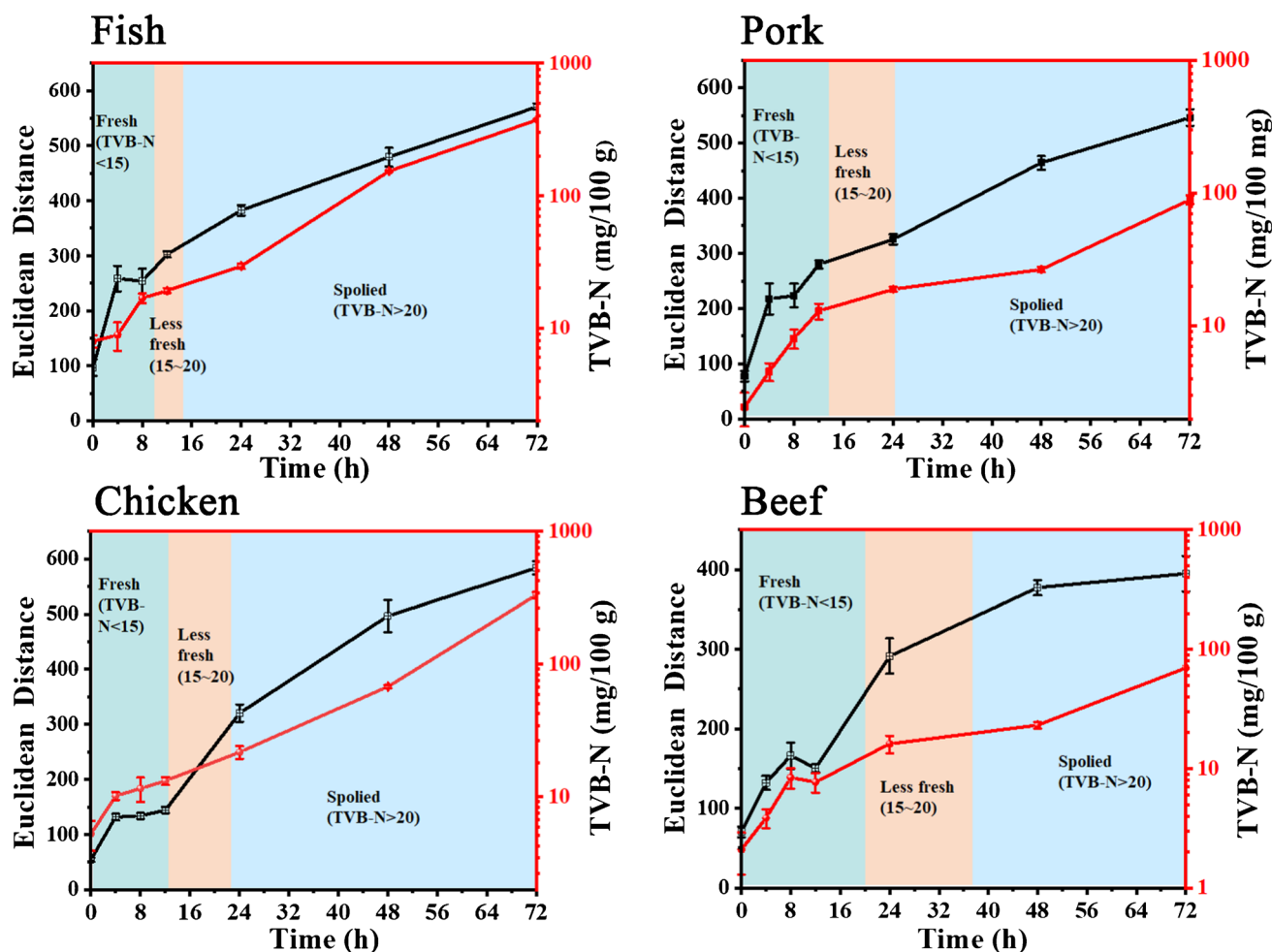


Fig. 7 Euclidean distance value and TVB-N content of meat samples at 25 °C over storage time. All measurements were performed four times

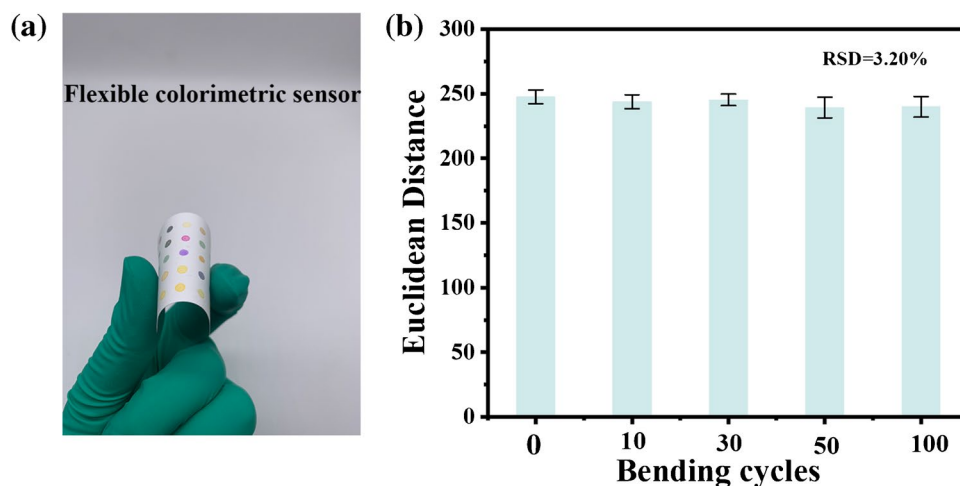
is inedible and spoiled [16, 44]. Figure 7 shows that the *ED* and TVB-N values of each sample increased during meat storage. According to the TVB-N values, the meat samples were classified into three grades (fresh, less fresh, and spoiled). We also integrated the colorimetric sensor array in a fish package that was stored under N₂ atmosphere, finding that the changes in both *ED* and TVB-N values were slower than those with air packaging (Fig. S8). This is attributed to the filling gas, nitrogen, which can hinder oxidative rancidity and growth of some microbes. Figure S9 shows the correlation between the *ED* value obtained from the sensor array and TVB-N content of meat during storage at 25 °C, which are in good agreement. Thus, it is fair to conclude that the flexible sensor array can be used as a simple alternative method for TVB-N in assessing meat freshness.

Reproducibility and stability

Reproducibility was explored using three different batches of sensor arrays to measure meat products four

times in succession. The results, shown in Fig. S10 and Table S3, reveal good repeatability, with relative standard deviations (RSD) below 5%, indicating that the prepared sensor array affords excellent reproducibility. The stability of the sensing response of the fully flexible colorimetric sensor against mechanical bending was also investigated, using DMA as the analyte. As shown in Fig. 8, during the cycling/bending test, almost no change in Euclidean distance was exhibited when the sensor was bent at an angle up to 180°, and no obvious deviation in response can be found after 100 bending cycles were applied. The results indicated good flexibility and reliability of the sensor (RSD = 3.2%). Additionally, the sensor also shows good long-term stability. After 4 weeks, the response to 25 ppm TMA maintained more than 85% of the initial response (Fig. S11). Nevertheless, one can find that the response gradually declined during storage, which may be related to passivation of the reactive sites on the sensor array due to adsorption of moisture or other species in the environment.

Fig. 8 Mechanical stability tests of the sensor array. **a** Photograph of a flexible colorimetric sensor. **b** The sensing responses toward 25 ppm DMA during bending tests



Conclusion

In conclusion, a novel, effective and nondestructive colorimetric sensor array was developed for the real-time and on-site assessment of meat product freshness. The sensor array resembles the mammalian olfactory system, which can sense volatiles released from rotting meat and form scent fingerprints. By extracting unique features, the sensor array can quickly identify four volatiles with detection limits down to the low ppb level. Moreover, the as-prepared colorimetric sensor array was applied to analyze meat samples, which further confirmed the practicability and reliability of the sensor. These results indicate that the colorimetric sensor array has great potential for monitoring food freshness and is a promising candidate for use in meat transport, storage, and consumption. It also serves as a useful alternative to other methods of food safety inspection.

Supplementary Information The online version contains supplementary material available at <https://doi.org/10.1007/s00216-022-04176-3>.

Acknowledgments This work was financially supported by the Key Program of the Natural Science Foundation of Shenzhen (JCYJ20200109113410174), the National Natural Science Foundation of China (81973280, 82173778), and Shenzhen Science and Technology Program (KQTD20170810105439418).

Author contributions **Wengui Nie:** Methodology, Formal analysis, Resources, Writing—original draft, Writing—review & editing. **Yifei Chen:** Formal analysis, Data curation, Methodology. **Hua Zhang:** Conceptualization, Methodology. **Jinsen Liu:** Software, Visualization. **Zhengchun Peng:** Validation, Supervision, Project administration, Writing—review & editing. **Yingchun Li:** Conceptualization, Validation, Investigation, Writing—review & editing, Funding acquisition.

Declaration

Competing of interest The authors declare that they have no competing interests.

References

- Liu T, Zhang W, Yuwono M, Zhang M, Su SW. A data-driven meat freshness monitoring and evaluation method using rapid centroid estimation and hidden Markov models. *Sensor Actuat B-Chem.* 2020;127868. <https://doi.org/10.1016/j.snb.2020.127868>.
- Ekmekcioglu C, Wallner P, Kundi M, Weisz U, Haas W, Hutter HP. Red meat, diseases, and healthy alternatives: A critical review. *Crit Rev Food Sci Nutr.* 2018;58(2):247–61. <https://doi.org/10.1080/10408398.2016.1158148>.
- Gui M, Liu L, Wu R, Hu J, Wang S, Li P. Detection of New Quorum Sensing N-Acyl Homoserine Lactones From *Aeromonas veronii*. *Front Microbiol.* 2018;9:1712. <https://doi.org/10.3389/fmicb.2018.01712>.
- Wang W, Feng X, Zhang D, Li B, Sun B, Tian H, et al. Analysis of volatile compounds in Chinese dry-cured hams by comprehensive two-dimensional gas chromatography with high-resolution time-of-flight mass spectrometry. *Meat Sci.* 2018;140:14–25. <https://doi.org/10.1016/j.meatsci.2018.02.016>.
- Petricevic S, Marusic Radovic N, Lukic K, Listes E, Medic H. Differentiation of dry-cured hams from different processing methods by means of volatile compounds, physico-chemical and sensory analysis. *Meat Sci.* 2018;137:217–427. <https://doi.org/10.1016/j.meatsci.2017.12.001>.
- Argyri AA, Jarvis RM, Wedge D, Xu Y, Panagou EZ, Goodacre R, et al. A comparison of Raman and FT-IR spectroscopy for the prediction of meat spoilage. *Food Control.* 2013;29(2):461–70. <https://doi.org/10.1016/j.foodcont.2012.05.040>.
- Chae I, Lee D, Kim S, Thundat T. Electronic Nose for Recognition of Volatile Vapor Mixtures Using a Nanopore-Enhanced Opto-Calorimetric Spectroscopy. *Anal Chem.* 2015;87(14):7125–32. <https://doi.org/10.1021/acs.analchem.5b00915>.
- Moudache M, Nerin C, Colon M, Zaidi F. Antioxidant effect of an innovative active plastic film containing olive leaves extract on fresh pork meat and its evaluation by Raman spectroscopy. *Food Chem.* 2017;229:98–103. <https://doi.org/10.1016/j.foodchem.2017.02.023>.
- Lin J-M, Huang Y-Q, Liu Z-b, Lin C-Q, Ma X, Liu J-M. Design of an ultra-sensitive gold nanorod colorimetric sensor and its application based on formaldehyde reducing Ag⁺. *RSC Adv.* 2015;5(121):99944–50. <https://doi.org/10.1039/c5ra16266a>.
- Gao M, Li S, Lin Y, Geng Y, Ling X, Wang L, et al. Fluorescent Light-Up Detection of Amine Vapors Based on

- Aggregation-Induced Emission. *ACS Sens.* 2015;1(2):179–84. <https://doi.org/10.1021/acssensors.5b00182>.
11. Huang XW, Zou XB, Shi JY, Li ZH, Zhao JW. Colorimetric Sensor Arrays Based on Chemo-Responsive Dyes for Food Odor Visualization. *Trends Food Sci Technol.* 2018;81:91–107. <https://doi.org/10.1016/j.tifs.2018.09.001>.
 12. Mma A, Nha C, Saa C, Ol B. Principles and recent advances in electronic nose for quality inspection of agricultural and food products. *Trends Food Sci Technol.* 2020;99:1–10. <https://doi.org/10.1016/j.tifs.2020.02.028>.
 13. Hou C, Li J, Huo D, Luo X, Dong J, Yang M, et al. A portable embedded toxic gas detection device based on a cross-responsive sensor array. *Sens Sensor Actuat B-Chem.* 2012;161(1):244–50. <https://doi.org/10.1016/j.snb.2011.10.026>.
 14. Li Z, Suslick KS. Portable Optoelectronic Nose for Monitoring Meat Freshness. *ACS Sens.* 2016;1(11):1330–5. <https://doi.org/10.1021/acssensors.6b00492>.
 15. Li Z, Li H, LaGasse MK, Suslick KS. Rapid Quantification of Trimethylamine. *Anal Chem.* 2016;88(11):5615–20. <https://doi.org/10.1021/acs.analchem.6b01170>.
 16. Guo L, Wang T, Wu Z, Wang J, Wang M, Cui Z, et al. Portable Food-Freshness Prediction Platform Based on Colorimetric Barcode Combinatorics and Deep Convolutional Neural Networks. *Adv Mater.* 2020;32(45):e2004805. <https://doi.org/10.1002/adma.202004805>.
 17. Gao Z, Ye H, Tang D, Tao J, Habibi S, Minerick A, et al. Platinum-Decorated Gold Nanoparticles with Dual Functionalities for Ultrasensitive Colorimetric in Vitro Diagnostics. *Nano Lett.* 2017;17(9):5572–9. <https://doi.org/10.1021/acs.nanolett.7b02385>.
 18. Wang X, Qin L, Zhou M, Lou Z, Wei H. Nanozyme Sensor Arrays for Detecting Versatile Analytes from Small Molecules to Proteins and Cells. *Anal Chem.* 2018;90(19):11696–702. <https://doi.org/10.1021/acs.analchem.8b03374>.
 19. Zeng J, Li M, Liu A, Feng F, Zeng T, Duan W, et al. Au/AgI Dimeric Nanoparticles for Highly Selective and Sensitive Colorimetric Detection of Hydrogen Sulfide. *Adv Funct Mater.* 2018;28(26). <https://doi.org/10.1002/adfm.201800515>.
 20. Wang G, Cai Z, Dou X. Colorimetric logic design for rapid and precise discrimination of nitrate-based improvised explosives. *Cell Rep Phys Sci.* 2021;2(2). <https://doi.org/10.1016/j.xcrp.2020.100317>.
 21. Wang G, Li Y, Cai Z, Dou X. A Colorimetric Artificial Olfactory System for Airborne Improvised Explosive Identification. *Adv Mater.* 2020;32(14):e1907043. <https://doi.org/10.1002/adma.201907043>.
 22. Zhang Y, Sharpee TO. A Robust Feedforward Model of the Olfactory System. *PLoS Comput Biol.* 2016;12(4):e1004850. <https://doi.org/10.1371/journal.pcbi.1004850>.
 23. Chiu SW, Tang KT. Towards a chemiresistive sensor-integrated electronic nose: a review. *Sensors (Basel).* 2013;13(10):14214–47. <https://doi.org/10.3390/s131014214>.
 24. Bushdid C, Magnasco MO, Vosshall LB, Keller A. Humans Can Discriminate More than 1 Trillion Olfactory Stimuli. *Sci.* 2014;343:1370–2. <https://doi.org/10.1126/science.1249168>.
 25. Pluskal T, Weng JK. Natural product modulators of human sensations and mood: molecular mechanisms and therapeutic potential. *Chem Soc Rev.* 2018;47(5):1592–637. <https://doi.org/10.1039/c7cs00411g>.
 26. Kida H, Fukutani Y, Mainland JD, de March CA, Vihani A, Li YR, et al. Vapor detection and discrimination with a panel of odorant receptors. *Nat Commun.* 2018;9(1):4556. <https://doi.org/10.1038/s41467-018-06806-w>.
 27. Guan B, Zhao J, Jin H, Lin H. Determination of Rice Storage Time with Colorimetric Sensor Array. *Food Anal Methods.* 2016;10(4):1054–62. <https://doi.org/10.1007/s12161-016-0664-6>.
 28. Lin H, Man ZX, Kang WC, Guan BB, Chen QS, Xue ZL. A novel colorimetric sensor array based on boron-dipyrromethene dyes for monitoring the storage time of rice. *Food Chem.* 2018;268:300–6. <https://doi.org/10.1016/j.foodchem.2018.06.097>.
 29. Liu X, Chen K, Wang J, Wang Y, Tang Y, Gao X, et al. An on-package colorimetric sensing label based on a sol-gel matrix for fish freshness monitoring. *Food Chem.* 2020;307:125580. <https://doi.org/10.1016/j.foodchem.2019.125580>.
 30. Liu B, Gurr PA, Qiao GG. Irreversible Spoilage Sensors for Protein-Based Food. *ACS Sens.* 2020;5(9):2903–8. <https://doi.org/10.1021/acssensors.0c01211>.
 31. Chen Y, Fu G, Zilberman Y, Ruan W, Ameri SK, Zhang YS, et al. Low cost smart phone diagnostics for food using paper-based colorimetric sensor arrays. *Food Control.* 2017;82:227–32. <https://doi.org/10.1016/j.foodcont.2017.07.003>.
 32. Salinas Y, Ros-Lis JV, Vivancos J-L, Martínez-Máñez R, Marcos MD, Aucejo S, et al. A novel colorimetric sensor array for monitoring fresh pork sausages spoilage. *Food Control.* 2014;35(1):166–76. <https://doi.org/10.1016/j.foodcont.2013.06.043>.
 33. Sun S, Qian S, Zheng J, Li Z, Lin H. A colorimetric sensor array for the discrimination of Chinese liquors. *Analyst.* 2020;145(21):6968–73. <https://doi.org/10.1039/d0an01496f>.
 34. Chen Q, Liu A, Zhao J, Ouyang Q, Sun Z, Huang L. Monitoring vinegar acetic fermentation using a colorimetric sensor array. *Sens Sensor Actuat B-Chem.* 2013;183:608–16. <https://doi.org/10.1016/j.snb.2013.04.033>.
 35. Weston M, Kuchel RP, Ciftci M, Boyer C, Chandrawati R. A polydiacetylene-based colorimetric sensor as an active use-by date indicator for milk. *J Colloid Interface Sci.* 2020;572:31–8. <https://doi.org/10.1016/j.jcis.2020.03.040>.
 36. Xiao-wei H, Xiao-bo Z, Ji-yong S, Zhi-hua L, Jie-wen Z. Colorimetric sensor arrays based on chemo-responsive dyes for food odor visualization. *Trends Food Sci Technol.* 2018;81:90–107. <https://doi.org/10.1016/j.tifs.2018.09.001>.
 37. Li Z, Askim JR, Suslick KS. The Optoelectronic Nose: Colorimetric and Fluorometric Sensor Arrays. *Chem Rev.* 2019;119(1):231–92. <https://doi.org/10.1021/acs.chemrev.8b00226>.
 38. Askim JR, Mahmoudi M, Suslick K. Optical sensor arrays for chemical sensing: the optoelectronic nose. *Chem Soc Rev.* 2013;42(22):8649–82. <https://doi.org/10.1039/c3cs60179j>.
 39. Chen HZ, Zhang M, Bhandari B, Yang CH. Novel pH-sensitive films containing curcumin and anthocyanins to monitor fish freshness. *Food Hydrocolloids.* 2019;100:105438. <https://doi.org/10.1016/j.foodhyd.2019.105438>.
 40. Zhao S, Lei J, Huo D, Hou C, Luo X, Wu H, et al. A colorimetric detector for lung cancer related volatile organic compounds based on cross-response mechanism. *Sens Sensor Actuat B-Chem.* 2017;256:543–52. <https://doi.org/10.1016/j.snb.2017.10.091>.
 41. Jon R, Askim Z, Li MK, LaGasse, et al. An optoelectronic nose for identification of explosives. *Chem Sci.* 2016;7:199–206. <https://doi.org/10.1039/C5SC02632F>.
 42. Bordbar MM, Tashkhourian J, Hemmateenejad B. Qualitative and quantitative analysis of toxic materials in adulterated fruit pickle samples by a colorimetric sensor array. *Sens Sensor Actuat B-Chem.* 2018;257:783–91. <https://doi.org/10.1016/j.snb.2017.11.010>.
 43. Mitchell L, New EJ, Mahon CS. Macromolecular Optical Sensor Arrays. *ACS Appl Polym Mater.* 2021;3(2):506–30. <https://doi.org/10.1021/acsapm.0c01003>.
 44. Lee H, Kim MS, Lee WH, Cho BK. Determination of the total volatile basic nitrogen (TVB-N) content in pork meat using hyperspectral fluorescence imaging. *Sens Sensor Actuat B-Chem.* 2018;259(APR):532–9. <https://doi.org/10.1016/j.snb.2017.12.102>.

Publisher's note Springer Nature remains neutral with regard to jurisdictional claims in published maps and institutional affiliations.



Wengui Nie is pursuing her master's degree in the Department of Pharmacy, Shihezi University. Her research focuses on the fabrication and application of functional materials and sensors.



Jinsen Liu is currently working at Shenzhen ENCO Instrument Co., Ltd. His work has focused on the research and development of bioanalytical instruments.



Yifei Chen is pursuing an MS degree in Pharmaceutical Analysis at Shihezi University. His research focuses on the fabrication and application of functional materials and colorimetric sensors.



Zhengchun Peng is a distinguished professor in the School of Physics and Optoelectronic Engineering at Shenzhen University. His main research interests are in the fields of micro/nano-sensors and flexible/stretchable electronics, and their application in robotics, health monitoring, and the human-machine interface.



Hua Zhang is Professor at the Department of Pharmacy, Shihezi University. Her research interests lie in Pharmaceutical Nanotechnology and the preparation and application of micro/nano-functional materials.



Yingchun Li received her B.S. from Shihezi University in 2003, and M.S. from Xi'an Jiaotong University in 2006. She continued her Ph.D. study at Halle University in Germany and received her doctoral degree in 2011. Then she joined Shihezi University as a scientist in the "Recruitment Program of Global Experts." Now, Prof. Li has continued her research at Harbin Institute of Technology (Shenzhen), and her research field is the development of advanced functional materials and sensors for serving pharmaceutical and biomedical analysis.